

THE PENNSYLVANIA STATE UNIVERSITY  
SCHREYER HONORS COLLEGE

DEPARTMENT OF BIOCHEMISTRY AND MOLECULAR BIOLOGY

IDENTIFYING INHIBITORS OF *TRANS*-TRANSLATION IN METHICILLIN RESISTANT  
*STAPHYLOCOCCUS AUREUS*

CHRISTOPHER RAE

SPRING 2015

A thesis submitted in partial fulfillment of the requirements  
for a baccalaureate degree in Biochemistry and Molecular Biology  
with honors in Biochemistry and Molecular Biology.

Reviewed and approved\* by the following:

Kenneth Keiler  
Associate Professor of Biochemistry and Molecular Biology  
Thesis Supervisor

Craig Cameron  
Professor of Biochemistry and Molecular Biology  
Honors Adviser

Scott Selleck  
Professor and Department Head of Biochemistry and Molecular Biology

\* Signatures are on file in the Schreyer Honors College.

## ABSTRACT

The development of antibiotic resistance among infectious bacteria is a serious public health problem. Methicillin resistant *Staphylococcus aureus* (MRSA) infections in particular have affected society for generations, demanding the need for new treatment options focused on previously untargeted mechanisms. The *trans*-translation pathway presents a good target for novel antibiotic development because it is universally conserved among bacteria and is essential for survival. This pathway uses two key components, SmpB and transfer-messenger RNA (tmRNA), which release stalled ribosome complexes that would otherwise accumulate and result in cell death. Identification of small molecule inhibitors against this pathway in MRSA has revealed a set of promising novel antibiotics that could one day treat this deadly infection.

Forty-six Kenneth Keiler Laboratory (KKL) compounds that inhibit *trans*-translation in *E. coli* were identified in a high-throughput screen. Broth microdilution assays showed that four of these compounds inhibit growth of *S. aureus* strains, including MRSA, at concentrations as low as 0.7  $\mu$ M. This is comparable to antibiotics in current use, such as vancomycin or clindamycin. All four compounds are oxadiazoles, characterized by a central five-membered heterocyclic ring and flanking phenyl derivatives. An *in vitro trans*-translation assay was established using *S. aureus* tmRNA and SmpB, and was used to evaluate the activity of these compounds. Inhibition of *trans*-translation was observed at levels nearing 25%. In contrast, no inhibition of translation was observed, indicating that these compounds specifically target *trans*-translation.

Bacterial cytological profiling (BCP) was adapted and optimized for use with suspected *trans*-translation inhibitors. BCP is a technique that takes advantage of the unique cell

morphologies that arise when bacteria are treated with antibiotics. Cell size and shape are visualized using fluorescence microscopy and quantified using image analysis software. Data can then be statistically compared and used to understand the cellular pathways targeted by various antibiotics. This technique was used to eliminate possible drug targets of KKL compounds, further suggesting that *trans*-translation is the target of inhibition.

These results indicate that *trans*-translation may serve as a target for the development of antibiotics to treat MRSA.

**TABLE OF CONTENTS**

LIST OF FIGURES .....	iv
LIST OF TABLES .....	v
ACKNOWLEDGEMENTS.....	vi
CHAPTER 1 Introduction .....	1
CHAPTER 2 In Vitro <i>trans</i> -Translation Assay .....	6
Background .....	6
Results.....	7
Discussion .....	11
Materials and Methods.....	13
CHAPTER 3 Bacterial Cytological Profiling .....	18
Background .....	18
Results.....	19
Discussion .....	22
Materials and Methods.....	23
APPENDIX Supplemental Information.....	26
BIBLIOGRAPHY .....	29

**LIST OF FIGURES**

Figure 1: trans-Translation.....	4
Figure 2: Structures of lead compounds. ....	8
Figure 3: In vitro <i>trans</i> -translation compatibility.....	9
Figure 4: In vitro <i>trans</i> -translation inhibition. ....	10
Figure 5: In vitro translation. ....	11
Figure 6: Antibiotic treated <i>E. coli</i> lptD4213 cell images. ....	20
Figure 7: Principle component analysis plot.....	21
Figure 8: Diagram of correlation between variables and factors. ....	28
Figure 9: Scree plot. ....	28

**LIST OF TABLES**

Table 1: Inhibitor activity against MRSA USA300-NRS384.....	7
Table 2: Inhibitor activity against <i>E. coli</i> lptD4213.....	19
Table 3: KKL Compounds.....	26
Table 4: Bacterial strains, plasmids and oligonucleotides.....	26
Table 5: Cell measurements.....	27

## **ACKNOWLEDGEMENTS**

Special thanks to Dr. Ken Keiler for your invaluable guidance and support. You have been an incredible mentor and I could not have asked for a more enjoyable and rewarding undergraduate research experience. Thanks to John Alumasa, Heather Feaga, Shaima El-Mowafi and all members of Keiler laboratory for their help and guidance. And thank you to my family for always being there for me.

## CHAPTER 1

### Introduction

The development of antibiotic resistance among infectious bacteria is a serious public health problem. Methicillin resistant *Staphylococcus aureus* (MRSA) infections in particular have affected society for generations, demanding the need for new treatment options focused on previously untargeted mechanisms. The *trans*-translation pathway presents a good target for novel antibiotic development because it is universally conserved among bacteria and is essential for survival. The goal of my project was to identify inhibitors of *trans*-translation in MRSA that may one day become antibiotics.

*Staphylococcus aureus* (*S. aureus*) is a spherical, gram positive bacterium which colonizes the skin and nostrils of nearly 30 percent of the human population.<sup>1,2</sup> *S. aureus* takes different pathogenic forms such as methicillin sensitive *S. aureus* (MSSA) and methicillin resistant *S. aureus*. MSSA is partially resistant to beta lactam antibiotics whereas MRSA is completely resistant. Beta lactam antibiotics includes penicillin and cephalosporin which were once the most commonly used antibiotics to treat *S. aureus* infections.

*S. aureus* causes a wide range of infections including skin and tissue infections, food poisoning, bacteremia, toxic shock syndrome and septic arthritis.<sup>3</sup> MRSA infections take similar forms however are more severe due to the increased difficulty of treatment. These infections may start as a minor scrape or pimple and become a serious and potentially fatal infection.<sup>4</sup> Treatment requires many doses of antibiotics and in severe cases, even surgery.<sup>5</sup>

MRSA infections, once confined within health care facilities, are becoming increasingly common within the community.<sup>6</sup> Healthcare associated MRSA infections are the result of exposure to the bacteria in a hospital setting.<sup>7</sup> Community associated MRSA on the other hand, is acquired by an individual who has not been recently hospitalized.<sup>7</sup> MRSA infections from both healthcare and community associated strains result in an estimated 80,000 invasive infections and 11,000 deaths every year in the United States.<sup>8</sup> With such a large number of infections and the continued emergence of community associated MRSA, the threat of increased antibiotic resistance is even greater.

Antibiotic resistance is the ability of a microorganism to withstand the effects of an antibiotic.<sup>8</sup> Bacteria gain antibiotic resistance either through random mutation and selection or the acquisition of resistance genes from other bacteria. In general, there are four ways bacteria deal with antibiotics: prevent entrance of the antibiotic into the cell; remove the antibiotic from the cell; mutate the antibiotic target; or inactivate the antibiotic itself.

Contributing to the increase in antibiotic resistance is the use, misuse and overuse of the antibiotics themselves. When antibiotics are used, an environment is created in which most bacteria die. A small number of bacteria may have a resistance mechanism allowing the cell to survive and replicate. This results in a bacterial strain with the ability to resist future antibiotic attack. Although this situation is unavoidable, there are human actions which accelerate the problem.

Individuals who do not complete their full course of antibiotic treatment in the recommended manner increase the likelihood of selecting for antibiotic resistance in bacteria.<sup>9</sup> Patients often don't complete their full course of treatment simply because they are already feeling better. Additionally, doctors may incorrectly prescribe antibiotics due to pressure from

patients, compounded by a lack of rapid diagnostic tests to verify bacterial illness. The excessive use of antibiotics in animal feed also contributes to an increase in antibiotic resistance. This seemingly beneficial action results in healthier livestock, but simultaneously selects for increasingly stronger bacteria to survive.<sup>9</sup>

Over the past sixty years, *S. aureus* has gained resistance to many antibiotics, including penicillin, methicillin and more recently against the once last-line antibiotic, vancomycin.<sup>10,11</sup> Drug-resistant *S. aureus* emerged shortly after the discovery and widespread use of penicillin in the late 1940's. Methicillin was invented and became popular in the late 1950's, and the first MRSA strains were identified only twelve years later.<sup>12</sup> More recently, in the late 1990's, *S. aureus* acquired resistance to vancomycin. These strains are known as vancomycin resistant *S. aureus* (VRSA).<sup>12</sup> The ability of *S. aureus* to quickly gain antibiotic resistance has affected society for decades, causing a perpetual demand for new treatment options.

Novel inhibitors aimed towards new targets must be identified for use as up-and-coming antibiotics. The *trans*-translation pathway presents a good target for novel antibiotic development because it is universal among bacteria, required for their survival and is found only within prokaryotes. These characteristics mean that inhibitors found to target this pathway have the potential to become safe, broad-spectrum antibiotics. Additionally, saturating mutagenesis studies have yet to reveal any resistant mutants to currently identified inhibitors. This result suggests that antibiotic resistance against these inhibitors would be slow to emerge.

*trans*-Translation functions as a quality control mechanism that releases stalled ribosomes unable to continue translation (Figure 1). These events occur frequently due to the translation of truncated or damaged mRNA lacking a stop codon. The two main components of *trans*-translation are a dual action transfer-messenger RNA (tmRNA) and an accessory protein,

SmpB.<sup>13</sup> tmRNA is a special RNA which acts initially as a tRNA, adding an alanine to the previously growing polypeptide, and then as an mRNA, where an open reading frame is translated by the ribosome. Translation of the open reading frame results in the addition of a sequence of amino acids which targets the protein for proteolysis.<sup>13</sup> This process frees the stalled ribosome, releases the mRNA and allows the polypeptide to be degraded in the cytoplasm. When *trans*-translation is inhibited, bacterial cells cease to grow, making the pathway a promising target for antibiotic development.<sup>14</sup>

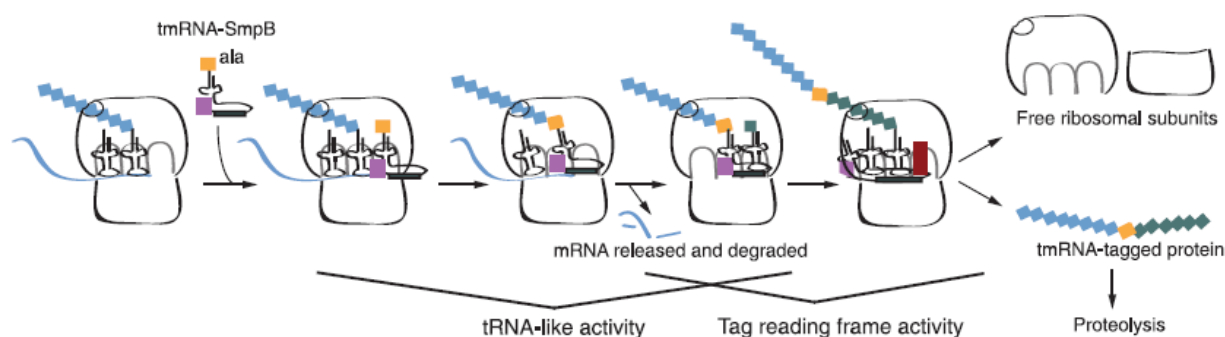


**Figure 1: trans-Translation.** trans-Translation releases all components of the non-stop ribosome complex. tmRNA-SmpB enter the A site after recognizing a stalled ribosome at the 3' end of an mRNA lacking a stop codon. An alanine carried by tmRNA is added to the nascent polypeptide and the tag reading frame is transferred to the mRNA decoding center where translation resumes using tmRNA as a message. Translation is then terminated via a stop codon in tmRNA. (Figure reproduced with permission.<sup>13</sup>)

Forty-six compounds that inhibit *trans*-translation in *E. coli* were identified in a high-throughput screen.<sup>14</sup> Due to the universal nature of *trans*-translation, inhibitors targeted against *E. coli* were hypothesized to show similar success against MRSA. Broth microdilution assays showed that four of these compounds inhibit growth of *S. aureus* strains, including MRSA, at concentrations as low as 0.7  $\mu\text{M}$ . This inhibitory concentration is comparable to antibiotics in

current use, such as vancomycin.<sup>15</sup> All four compounds are oxadiazoles, characterized by a central five-membered heterocyclic ring and flanking phenyl derivatives.

An in vitro *trans*-translation assay was established using *S. aureus* tmRNA and SmpB and was used to evaluate the activity of these compounds. Inhibition of *trans*-translation was observed at levels nearing 25%. In contrast, no inhibition of translation was observed, indicating that these compounds specifically target *trans*-translation.

Bacterial cytological profiling (BCP) was adapted and optimized for use with suspected *trans*-translation inhibitors. BCP is a technique which takes advantage of the unique cell morphologies that arise when bacteria are treated with antibiotics.<sup>16</sup> Cell size and shape are visualized using fluorescent microscopy and quantified using image analysis software. Data can then be statistically compared and used to understand the cellular pathways targeted by various antibiotics. This technique was used to eliminate possible drug targets of KKL compounds, further suggesting that *trans*-translation is the target of inhibition.

These results indicate that *trans*-translation may serve as a target for the development of antibiotics to treat MRSA.

## CHAPTER 2

### In Vitro *trans*-Translation Assay

#### Background

*Origin of inhibitors: high throughput screening*<sup>14</sup>

A cell-based high throughput screening (HTS) assay was used to detect possible inhibitors of *trans*-translation in *E. coli*. This screen uses an *E. coli* strain constructed with the firefly luciferase gene, *luc*, inserted into the chromosome. *luc* encodes a luciferase enzyme which produces detectable luminescence in the presence of its substrate, luciferin. A *trpAt* transcriptional terminator was added before the stop codon of this gene and as a result, mRNA lacking a stop codon is produced when *luc* transcription is induced. Non-stop complexes are formed in the cells due to the translation of these mRNA's. The non-stop complexes are resolved by *trans*-translation, resulting in the degradation of luciferase and consequently the absence of luminescence. In the presence of a *trans*-translation inhibitor, luciferase is not degraded and therefore luminescence is detected.

Six hundred sixty-three thousand compounds were screened using this method, revealing 178 possible inhibitors of *trans*-translation. This screen was completed in collaboration with the Genomics Institute of the Novartis Research Foundation. Forty-six compounds were chosen for further investigation, and 12 were available for use with MRSA.

## Results

### *Identification of inhibitors effective against MRSA*

Broth microdilution assays were performed using MRSA USA300-NRS384, a particularly virulent strain of drug resistant *S. aureus*. Four inhibitors showed especially outstanding results: KKL-35, KKL-10, KKL-40, KKL-52 (Table 1, Figure 2). These compounds have minimum inhibitory concentrations (MIC) equal to or better than current antibiotics, such as vancomycin or clindamycin (Table 1). The four lead compounds were selected to undergo secondary screening using a *trans*-translation assay.

**Table 1:** Inhibitor activity against MRSA USA300-NRS384

Compound	MIC* ( $\mu$ M)
KKL-40	0.65 $\pm$ 0.13
KKL-35	0.78 $\pm$ 0.00
KKL-52	1.07 $\pm$ 0.34
KKL-10	1.30 $\pm$ 0.26
KKL-55	7.8 $\pm$ 0.00
KKL-22	12.5 $\pm$ 0.00
KKL-87	21.88 $\pm$ 3.6
KKL-96	25 $\pm$ 0.00
KKL-69	25 $\pm$ 0.00
KKL-73	> 25
KKL-74	> 25
KKL-66	> 25
Vancomycin	0.69
Clindamycin	1.18
Tetracycline	4.50
Erythromycin	5.45

\*Data represent the average and standard deviation of three independent repeats.

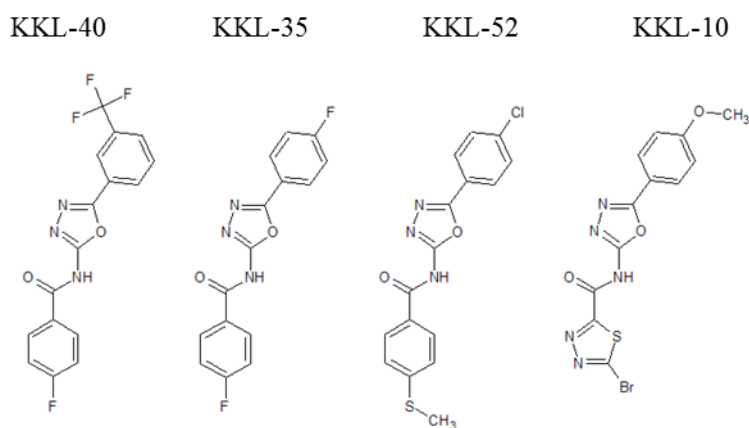


**Figure 2: Structures of lead compounds.** The four lead compounds are oxadiazoles, characterized by a central five-membered heterocyclic ring. Phenyl or heterocyclic ring derivatives are attached to the central ring either directly or through an amide linkage. Variation of phenyl group substituents results in differing activities within the cell.

#### *In vitro trans-translation assay verifies trans-translation inhibition in MRSA*

An *in vitro trans-translation* assay was adapted to screen lead compounds for activity against *trans-translation*. Protein synthesis reactions were developed, incorporating *trans-translation* activity from MRSA tmRNA-SmpB. This is the first time tmRNA and SmpB were purified from a *S. aureus* strain and the first demonstration that these components are actively compatible with *E. coli* ribosomes and translation factors.

The genes for *S. aureus* tmRNA and SmpB, *ssrA* and *smpB*, respectively, were amplified from genomic DNA of MRSA USA300F and cloned into a plasmid. From this plasmid, *smpB* was amplified and cloned into an expression vector which was transformed into *E. coli*. SmpB protein was overexpressed, harvested and then purified using nickel-affinity and ion exchange chromatography. *ssrA* was amplified from the original plasmid, and tmRNA was synthesized by *in vitro* transcription. tmRNA was purified by gel electrophoresis extraction.

Protein synthesis reactions were developed using purified MRSA tmRNA-SmpB and *E. coli* transcription and translation machinery along with non-stop dihydrofolate reductase (nsDHFR) DNA template lacking a stop codon. These reactions result in the production of stalled ribosome complexes containing DHFR protein. When *trans*-translation is active, the stalled complexes are rescued and the reactions result in “tagged” 20.4 kDa DHFR protein. In the presence of *trans*-translation inhibitors, the polypeptide tag is not added, resulting in a shorter 19.2 kDa protein. These newly synthesized protein bands are detected using <sup>35</sup>S-Methionine, a radiolabeled amino acid incorporated only into the newly synthesized DHFR protein.

During assay development, MRSA tmRNA-SmpB were shown to be compatible with purchased *E. coli* ribosomes and translation factors. *trans*-Translation activity was increased by 37% after the addition of MRSA tmRNA- SmpB (Figure 3).

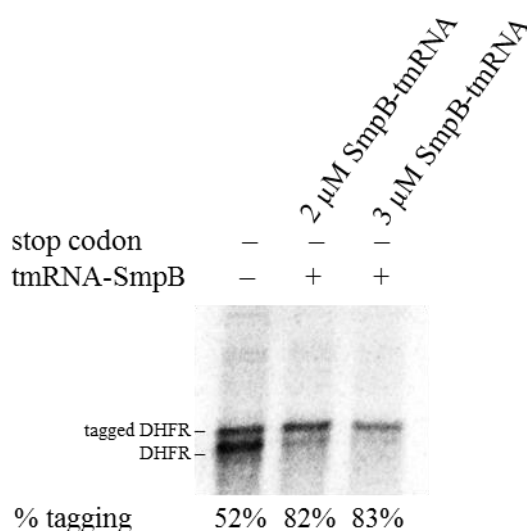


**Figure 3: In vitro *trans*-translation compatibility.** The protein production reactions developed in this study demonstrate for the first time that tmRNA-SmpB from one genus can be actively compatible with ribosomes and translation factors of another. Reactions were tested with two different concentrations of tmRNA-SmpB, both showing the ability to increase *trans*-translation activity from that inherently present due to ribosome preparation methods.

The two best lead compounds, KKL-35 and KKL-40, were tested using this assay. Both compounds inhibited MRSA *trans*-translation in vitro. Tagging activity was decreased by 13.3% in KKL-35 treated reactions and 22.9% in KKL-40 treated reactions (Figure 4).

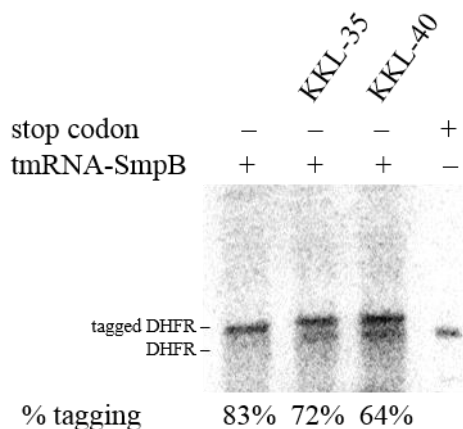


**Figure 4: In vitro *trans*-translation inhibition.** 10.3  $\mu$ M treated KKL-35 (lane 2) and KKL-40 (lane 3) reactions both resulted in an increase in untagged DHFR band intensity. A control reaction without inhibitor added shows maximum *trans*-translation activity (lane 1). A second control reaction using DHFR template containing a stop codon and no added tmRNA-SmpB demonstrates pure translation activity.

In vitro translation reactions without the addition of tmRNA-SmpB showed that translation is not inhibited by either KKL-35 or KKL-40 (Figure 5a). These reactions use DHFR template DNA containing a stop codon and, when uninhibited, result in successful translation and formation of 19.2 kDa DHFR protein. Chloramphenicol was used as a control for translation inhibition. The relative translation activity was quantified based on normalized band intensity and, interestingly, it appears that translation is increased compared to the DMSO-treated control (Figure 5b).

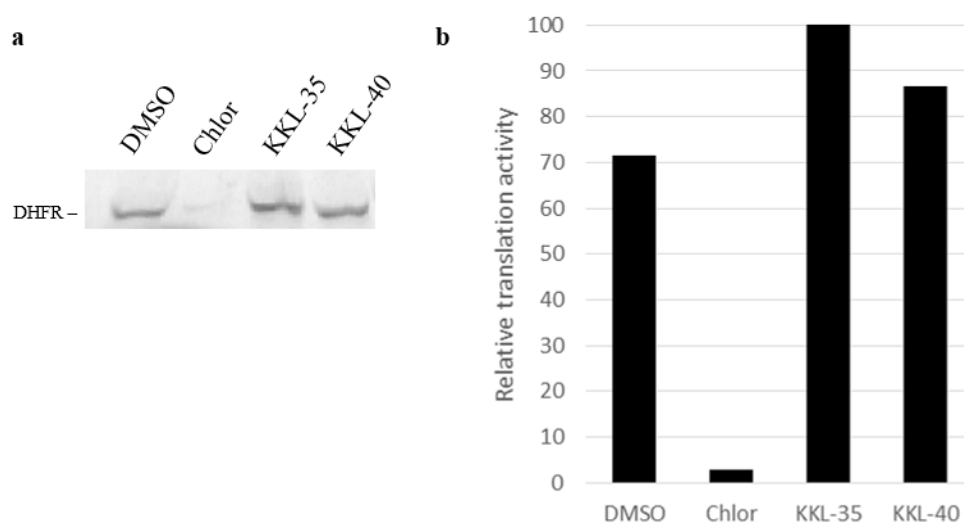


**Figure 5: In vitro translation.** The quantified band intensities of the KKL-35 and KKL-40 treated reactions show that translation is not inhibited and is actually increased compared to the DMSO control reaction. Inhibitors and chloramphenicol were tested at 70  $\mu$ M. This assay was only completed once, therefore, additional trials are needed to confirm these results.

## Discussion

Due to the conserved nature of *trans*-translation, compounds suspected of inhibiting *trans*-translation in *E. coli* were hypothesized to be effective against MRSA. These compounds were tested using broth microdilution assays and four were shown to have outstanding inhibitory effects. This exciting result means that these compounds have the properties necessary to enter the bacterial cell and inhibit cell growth.

To determine if the cause of growth inhibition was due to the inhibition of *trans*-translation, an in vitro *trans*-translation assay was developed. The results of this assay show that *trans*-translation and not translation is inhibited in MRSA. Because a decrease in percent tagging is observed (Figure 4), the compounds are likely inhibiting a step that is directly involved with the function of tmRNA, SmpB, EF-Tu or the non-stop ribosome complex and not a downstream

result of *trans*-translation such as proteolysis. Nonstop complex resolution is essential for survival, and *trans*-translation is the bacterial cell's primary means of doing so. Therefore, since these compounds target *trans*-translation, antibiotic resistance is likely to be slow to develop.

The *trans*-translation assay uses a mixture of both *E. coli* and MRSA components yet still yields adequate *trans*-translation activity (Figure 3). This speaks to the universal nature of this pathway and reinforces its conservation among all bacteria. However, due to the manner in which *E. coli* ribosomes are prepared for the purchased kit, there is a variable amount of endogenous *trans*-translation activity. More strongly conclusive evidence for the claim of *trans*-translation inhibition in MRSA will come from the preparation of a MRSA ribosome lysate used in conjunction with a protein expression system lacking the *E. coli* ribosomes.

Chloramphenicol was used as a control translation inhibitor. This antibiotic inhibits peptidyl transferase of the 50S ribosome.<sup>16</sup> *trans*-Translation requires this activity to add the peptide sequence which targets the nascent polypeptide for proteolysis. The results, therefore, suggest that these compounds are not inhibiting *trans*-translation in this manner otherwise translation would also be inhibited. The mechanism of action must therefore be intimately related to the interference with the known components of *trans*-translation and the specific conformation of the non-stop ribosome.

It appears that both KKL-35 and KKL-40 increase translation activity relative to an equal amount of DMSO (Figure 5). This is consistent with the observation that the total protein content for KKL-35 and KKL-40 treated *trans*-translation reactions is greater than the untreated control (Figure 4). In some way, these compounds seem to increase translation activity yet simultaneously decrease *trans*-translation activity. Additional replicates of this experiment are

necessary to confirm the results. The mechanism of these inhibitors may one day be understood through discovery of the molecular structures of compound-bound target molecules.

These results inspire further inquiry into the mechanism of *trans*-translation inhibition in MRSA and show promise for the future development of KKL compounds as potential antibiotics.

## Materials and Methods

### *Compounds*

Kenneth Keiler Laboratory (KKL) compounds were obtained at 1 mM in DMSO. Compounds originated from high throughput screening conducted in collaboration with the Genomics Institute of the Novartis Research Foundation.

### *Bacterial Strains*

*S. aureus* strain MRSA USA300-NRS384 was used for MIC assays. Genomic DNA was obtained from *S. aureus* strain USA300F through generous donation by Mike Mwangi, Penn State University. Various *E. coli* strains were used for cloning and are detailed in the appendix, Table 4. All strains were grown at 37°C in lysogeny broth. Antibiotics, 30 µg/mL kanamycin or 50 µg/mL ampicillin, were added to growth media when necessary.

### *Minimum inhibitory concentration assay*

Broth microdilution assays were performed following standard protocol.<sup>17</sup> Bacteria were grown overnight and the next day, diluted to OD<sub>600</sub> = 0.001 (approximately 5 x 10<sup>5</sup> colony

forming units (cfu)/mL). Inhibitors were added to lysogeny broth and serially diluted in 96 well microtiter plates. Cells were added to the dilutions and the plate was incubated for 24 h at proper growth temperature for respective strain (Table 4). The MIC was identified as the lowest concentration of inhibitor at which no growth was observed.

### *Plasmids and Cloning*

Two plasmids were created for this study. All plasmids and oligonucleotide primers are detailed in the appendix, Table 3.

The first plasmid, pCDR1, contains MRSA USA300F *smpB-ssrA* genes in pGEM T-easy vector (Promega). MRSA *smpB-ssrA* was amplified from genomic DNA using Polymerase Chain Reaction (PCR) with MRSA F2 and MRSA R2 primers, and One Taq DNA Polymerase (New England BioLabs). This PCR product was ligated into pGEM T-easy vector using T4 DNA ligase (New England BioLabs) and the pGEM T-easy kit (New England BioLabs). The resulting plasmid was named pCDR1 and transformed into *E. coli* DH5 $\alpha$ . Blue-white screening on lysogeny broth plates containing ampicillin, isopropyl-beta-D-thiogalactopyranoside (IPTG), and 5-bromo-4-chloro-3-indolyl-beta-D-galacto-pyranoside (XGal) was used to isolate cells containing pCDR1. pCDR1 was prepared from these colonies and sequenced at the Genomics Core Facility, University Park Pennsylvania.

The second plasmid, pCDR2, contains His tagged MRSA USA300F *smpB* in pET28a vector. In this plasmid, *smpB* is under control of an IPTG inducible T7 RNA polymerase promoter. MRSA *smpB* was amplified from pCDR1 using PCR with *smpBGibF* and *smpBGibR* primers, and Q5 High-fidelity DNA Polymerase (New England BioLabs). pET28a was isolated from *E. coli* KCK101 and restriction digested with Bam H1 and Nde1 fast digest enzymes (New

England BioLabs). The PCR product and digested pET28a vector were ligated using TA cloning via Gibson Assembly reaction (New England BioLabs). The resulting plasmid, named pCDR2, was transformed into *E. coli* DH5 $\alpha$  and grown on lysogeny broth plates containing kanamycin. Colonies containing pCDR2 were harvested and plasmid content confirmed using colony PCR.

### *SmpB Expression and Purification*

pCDR2 was transformed into *E. coli* expression strain KCK28-BL2IDE3 and grown in 1 L terrific broth with kanamycin. Cells were grown to OD<sub>600</sub> = 0.6, induced with IPTG and then harvested by centrifugation (10 min, 8000 rpm, 4°C) after 3 h. Cells were suspended in Wash Buffer (50 mM NaH<sub>2</sub>PO<sub>4</sub> pH 8.0, 300 mM NaCl, 20 mM imidazole). 1 mg/mL lysozyme was added and the sample was incubated for 1 h on ice. Cells were then lysed using sonication and cleared by centrifugation (5 min, 12000 rpm, 4°C). Cleared lysate was incubated overnight with 0.1% (v/v) Ni-NTA resin (Qiagen). The resin-lysate mixture was poured into a column and washed with 100 bed volumes of Wash Buffer. SmpB was eluted with Elution Buffer (50 mM NaH<sub>2</sub>PO<sub>4</sub> pH 7.6, 300 mM NaCl, 500 mM imidazole) and detected by SDS-PAGE. Fractions were pooled and dialyzed against Buffer A (50 mM HEPES.KOH pH7.6, 100 mM KCl, 10 mM MgCl<sub>2</sub>, 7 mM 2-Mercaptoethanol). The SmpB sample was then added to an anion exchange column (MonoS HR 5/5, GE Healthcare). The column was washed with Buffer A and SmpB was eluted using a linear gradient from 100 – 1000 mM KCl. The sample was stored in 10% glycerol at -80°C.

### *tmRNA Synthesis and Purification*

MRSA *ssrA* was amplified from pCDR1 using PCR with MRSAssrAF and MRSAssrAR2, and Q5 High-fidelity DNA Polymerase (New England BioLabs). In vitro transcription reactions containing 100 mM Hepes.KOH, pH 7.5, 3 mM MgCl<sub>2</sub>, 10 mM DTT, 2 mM spermidine, 30 mM NTP mix (ATP, UTP, CTP, and GTP, pH 7; Sigma), 2 U/mL inorganic pyrophosphatase, 10 µg/mL purified PCR product, and 10 µg/mL T7 RNA polymerase were incubated for 3 h at 37 °C. Reactions were treated with 40 U/mL DNase I and incubated at 37°C for 10 min. Treatment was terminated by adding ethylenediaminetetraacetic acid (EDTA) (5 mM final concentration) and incubating at 75°C for 10 min. The synthesized MRSA tmRNA was run on a 5% denaturing Sequa Gel (National Diagnostics) and detected by UV shadowing. Bands were cut from the gel and tmRNA eluted with Diffusion Buffer (0.5 M NH<sub>4</sub>OAc, 1 mM EDTA, 0.2% w/v SDS) by incubating at 37°C overnight. tmRNA was precipitated by adding sodium acetate (3 mM final concentration) and an equal volume of 200 proof ethanol. tmRNA was pelleted (10 min, 14000 rpm, 4°C) and washed with 80% ethanol. The pellet was incubated at room temperature for 45 min to dry and then suspended in water. tmRNA was refolded by heating to 95°C for two minutes and slowly cooling to 4°C, then stored at -20°C. All processes were conducted under RNase free conditions.

### *In vitro translation and trans-translation assays*

In vitro translation was completed using PURExpress protein synthesis kit (New England BioLabs) according to manufacturer's protocol. Inhibitors and chloramphenicol were tested at 70 µM concentrations and DMSO at 7%. <sup>35</sup>S-Methionine was added to the reactions to detect newly synthesized proteins by exposure to a phosphor screen. Reactions were run on 12% SDS-PAGE,

the gel dried and then exposed to a phosphor screen. The phosphor screen was then scanned and band intensities quantified using ImageQuant (GE Healthcare Life Sciences).

In vitro *trans*-translation was tested using the same kit with the addition of purified MRSA tmRNA and SmpB at 2  $\mu$ M final concentrations. nsDHFR was used in the reactions at 40  $\mu$ g/mL final concentration. nsDHFR was produced using PCR with PURExpress Universal and DHFR Rev UTR primers and Phusion high fidelity DNA Polymerase (Thermo). Translation controls were made with full length DHFR template (New England BioLabs). Inhibitors were tested at 10.3  $\mu$ M final concentrations. Individual band intensities were first normalized based on area. Tagging activity was calculated as the intensity of the tagged band divided by the sum of the intensities of both the tagged and untagged bands.

## CHAPTER 3

### Bacterial Cytological Profiling

#### Background

##### *Origin of procedure*

The novel technique described in Joe Pogliano's 2013 paper, "Bacterial cytological profiling rapidly identifies the cellular pathways targeted by antibacterial molecules", was adapted for use in Keiler Laboratory. A bacterial cytological profiling (BCP) protocol was developed and optimized to aid in target pathway identification for suspected *trans*-translation inhibitors.

##### *Technique fundamentals*

BCP is a technique used to predict pathways targeted by antibiotics and is based on the measurement of changes in cell morphology in response to antibiotic treatment. A special strain of *E. coli* is used in this technique which has a mutated outer membrane  $\beta$ -barrel causing it to become "leaky" and exaggerate the morphological changes resulting from antibiotic treatment.

The differences in cell size and shape after antibiotic treatment can be visualized using fluorescent microscopy and quantified via image analysis software. This information is statistically analyzed using principle component analysis (PCA), where data is manipulated in a way that can be represented on two dimensional scatter plot. Data points representing specific

antibiotic treatments group together and can be differentiated from other antibiotic treatment groups in distinct areas of the scatter plot.

## Results

### *Minimum inhibitory concentrations*

MIC's for the four lead *trans*-translation inhibitors were measured (Table 2). Control antibiotics are also reported. Knowing the MIC allows for consistency between antibiotic treatments. This means that cells are placed under similar levels of stress by each inhibitor even though in reality some are more effective than others.

**Table 2:** Inhibitor activity against *E. coli* lptD4213

Compound	MIC* ( $\mu\text{M}$ )
KKL-10	$0.78 \pm 0.00$
KKL-35	$1.56 \pm 0.00$
KKL-40	$0.78 \pm 0.00$
KKL-52	$1.56 \pm 0.00$
Ampicillin**	0.57
Ciprofloxacin	0.015
Tetracycline	1.13
Rifampicin	0.006
Triclosan	0.014

\*Data represent the average and standard deviation of two independent repeats.

\*\*All antibiotic data were obtained from source (16).

### Cell imaging

Cells treated with antibiotics or KKL compounds were imaged using fluorescent microscopy (Figure 6). Three stains were used: FM4-64 to bind the cell membrane; DAPI to bind DNA in living or dead cells; and Sytox Green to bind DNA in dead cells. The drastic differences between ciprofloxacin, ampicillin and the other antibiotics are easily observed. Both ciprofloxacin and ampicillin have elongated cell shapes but ciprofloxacin has a more condensed nucleoid whereas ampicillin treated cells have a decondensed nucleoid region. Subtle differences between tetracycline, rifampicin, triclosan and the untreated cells are more difficult to recognize. Tetracycline treated cells are slightly smaller than the others and rifampicin treated cells are slightly larger. Triclosan tends to result in the formation of pairs of incompletely divided cells. KKL treated cells are similar in shape to the untreated control cells.

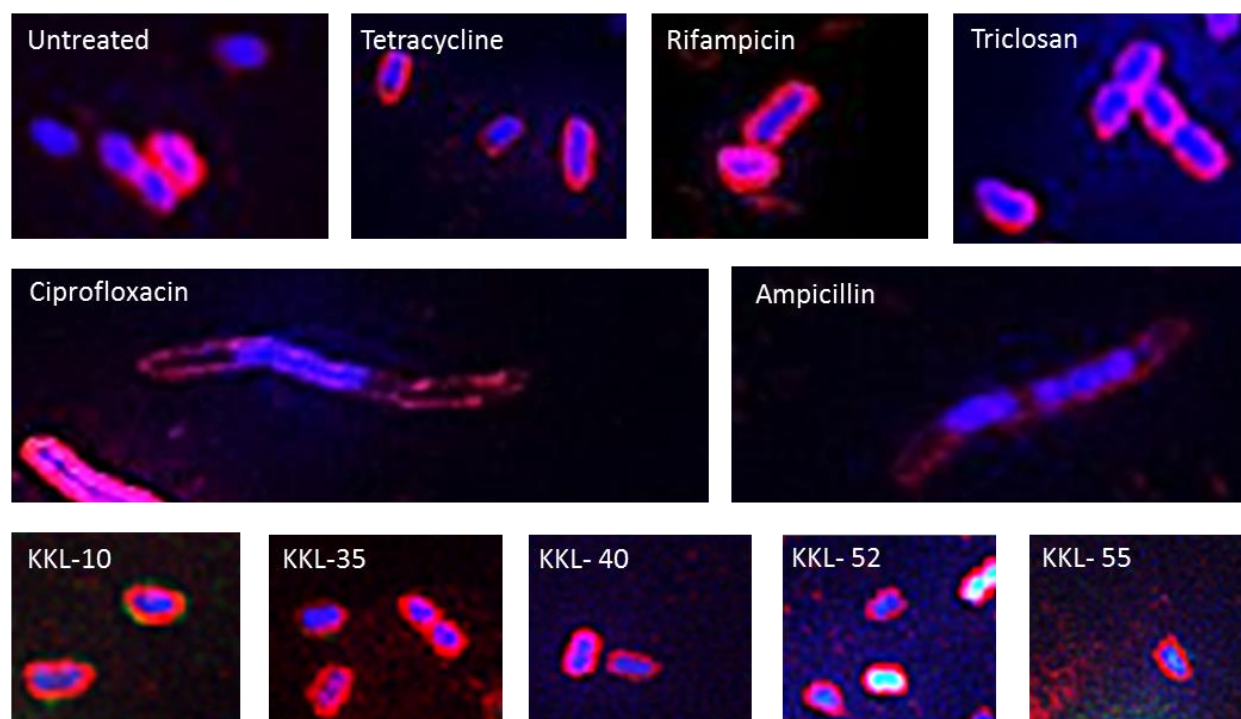


**Figure 6: Antibiotic treated *E. coli* lptD4213 cell images.** After treating cells with 5X MIC of antibiotic for two hours, cells were fluorescently stained and visualized by microscopy.

### *Bacterial cytological profiling helps eliminate major drug target possibilities*

Principal component analysis of averaged cell measurements (Table 5, Appendix) revealed clustering of the data points on a two dimensional scatter plot representing repeat antibiotic treatments (Figure 7). Ampicillin and ciprofloxacin data points are well separated from other antibiotics as would be expected due to their obvious morphological differences. Rifampicin, tetracycline and triclosan begin to overlap and cannot be accurately distinguished from one another. “Untreated” data points, representing cells treated with either water, DMSO, or ethanol (the solvents for the antibiotics) group more tightly. KKL-compounds slightly overlap in the control, rifampicin and tetracycline data point regions, however still appear to have a relative territory of their own.

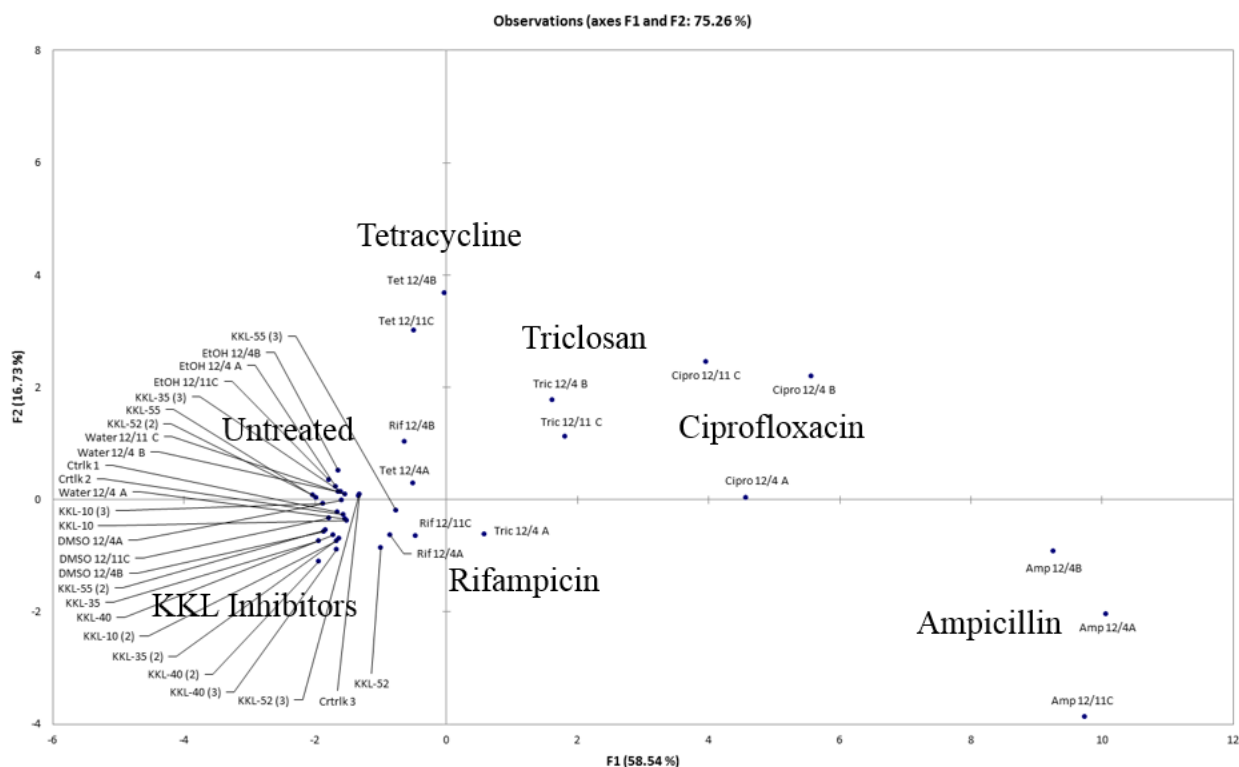


**Figure 7: Principle component analysis plot.** Cell measurements were averaged for each treatment repeat and statistically analyzed using PCA. This technique allows the measurements of individual treatments to be viewed on a scatter plot as a single data point.

A diagram (Figure 8) showing the correlation between variables and factors, and a scree plot (Figure 9) showing the eigenvalue associated with each factor and cumulative variability of all factors in the PCA are presented in the appendix.

## Discussion

The five control antibiotics used in BCP target different cellular pathways. Ampicillin targets penicillin-binding proteins resulting in the inhibition of cell wall peptidoglycan synthesis.<sup>16</sup> Ciprofloxacin targets DNA gyrase A, inhibiting DNA synthesis.<sup>16</sup> Tetracycline binds to the 30S ribosomal subunit inhibiting protein synthesis.<sup>16</sup> Rifampicin inhibits DNA-dependent RNA polymerase and therefore stops RNA transcription.<sup>16</sup> Lastly, triclosan binds bacterial enoyl-acyl carrier protein reductase, inhibiting lipid synthesis.<sup>16</sup>

These five major processes are those inhibited by many antibiotics in current use today. *trans*-Translation has never been targeted before and it was therefore hypothesized that data points representing KKL compound-treated cells would fall into their own grouping, defining a new class of inhibitory compounds. BCP has shown that the target of KKL compounds is likely not the same as those of ampicillin, ciprofloxacin, triclosan, tetracycline, or rifampicin based on the lack of completely overlapping data clusters.

This conclusion is based on the prediction that if one antibiotic acts on the same pathway as another, cell morphology would be the same and therefore the resulting data points would overlay completely in the scatter plot. This prediction is well supported by the fact that, although not in this study, data points representing compounds with similar mechanisms of inhibition have been shown by Pogliano et al. to group together on two dimensional plots.<sup>16</sup>

It was unexpected that tetracycline, rifampicin and triclosan data points would overlap. Limitations due to magnification and cell measuring software likely resulted in the overlap of the rifampicin, tetracycline, and triclosan territories. It is predicted that with an increase in technological capabilities and further optimization of the technique, these discrepancies will be resolved and BCP will become a powerful tool used to screen suspected *trans*-translation inhibitors.

With an increase in biochemical data advancing our understanding of *trans*-translation inhibitors, this technique has the potential to become a tool for quickly investigating the mechanism of action of compounds suspected of targeting *trans*-translation.

## **Materials and Methods**

### *Antibiotics and inhibitors*

Tetracycline, rifampicin, triclosan, ciprofloxacin, and ampicillin (Sigma Aldrich) were prepared according to manufacturer recommendations. KKL compounds were obtained at 1 mM in DMSO originating from high throughput screening conducted in collaboration with the Genomics Institute of the Novartis Research Foundation.

### *Bacterial strain*

*E. coli* lptD4213 was obtained by generous donation from Joe Pogliano, University of California San Diego. This strain was grown in lysogeny broth at 30°C for all assays.

### *Minimum inhibitory concentration assays*

Broth microdilution assays were performed following standard protocol as described in Chapter 2 Materials and Methods.

### *Bacterial growth and antibiotic treatment*

Overnights were diluted 1:100 and grown to  $OD_{600} = 0.600$  in a shaking water bath. The culture was separated, treated with compounds at 5X MIC and incubated for 2 hours. Cells were fluorescently stained with 1  $\mu\text{g}/\text{mL}$  FM4-64, 2  $\mu\text{g}/\text{mL}$  DAPI and 0.5  $\mu\text{M}$  Sytox Green (Molecular Probes/Invitrogen) and incubated for 7 min at 30°C. Cells were pelleted (1 min, 14000 rpm) and then suspended in water.

### *Fluorescent microscopy and cell morphology measurements*

3  $\mu\text{L}$  of fluorescently stained cells were added to an agarose pad (1.2% agarose, 20% LB) and viewed with 60X objective on a Nikon Eclipse 90i microscope. Exposure time remained constant for every repeat of the experiment. Images were captured with a Photometrics CoolSNAP HQ camera and analyzed using SimplePCI software version 6.6.0 (CImaging Systems). Using quantitative fluorescence analysis, polygons were drawn around every visible cell in the imaging field based on the membrane or nucleoid. Polygons were then measured using ROI shapes.

### *Principal component analysis*

Cell measurements ( $n > 30$ ) were averaged for each repeated treatment (Table 5, Appendix). Statistical analysis of this data was completed using XLSTAT version 2014.4.09

with Microsoft Excel for Windows 7. Principal component analysis using Spearman rank correlation and unweighted variables was used to create two dimensional scatter plots of the cell morphology measurements.

## APPENDIX

## Supplemental Information

Table 3: KKL Compounds

Abbreviation	Full Chemical Name
KKL-35	4-chloro- <i>N</i> -[5-(4-fluorophenyl)-1,3,4-oxadiazol-2-yl]benzamide
KKL-10	5-bromo- <i>N</i> -[5-(4-methoxyphenyl)-1,3,4-oxadiazol-2-yl]thiophene-2-carboxamide
KKL-55	3-chloro- <i>N</i> -(1-propyl-1 <i>H</i> -tetrazol-5-yl)benzamide
KKL-40	<i>N</i> -[5-(4-fluorophenyl)-1,3,4-oxadiazol-2-yl]-3-(trifluoromethyl)benzamide
KKL-22	3-bromo- <i>N</i> -[5-(furan-2-yl)-1,3,4-oxadiazol-2-yl]benzamide
KKL-96	<i>N</i> -(3-bromophenyl)-5-nitrothiophene-2-carboxamide
KKL-69	5-bromo- <i>N</i> -(3-fluorophenyl)thiophene-2-carboxamide
KKL-52	<i>N</i> -[5-(4-chlorophenyl)-1,3,4-oxadiazol-2-yl]-4-(methylsulfanyl)benzamide
KKL-73	5-nitroquinolin-8-yl 3-(morpholin-4-ylsulfonyl)benzoate
KKL-66	5-chloro- <i>N</i> -cyclopentylthiophene-2-carboxamide
KKL-74	3-chloro-9 <i>H</i> -carbazole
KKL-87	<i>N</i> -(quinolin-8-yl)thiophene-2-sulfonamide

Table 4: Bacterial strains, plasmids and oligonucleotides

Name	Description	Source
<i>Escherichia coli</i>		
DH5 $\alpha$	High yield transformation strain	
KCK101	Contains pET28a, Kan <sup>r</sup>	
KCK28 - BL21DE3	Expression strain	
CDR1	DH5 $\alpha$ with pCDR1, Amp <sup>r</sup>	This study
CDR2	KCK28-BL21DE3 with pCDR2, Kan <sup>r</sup>	This study
lptD4213	BCP strain, increased membrane permeability	16
<i>Staphylococcus aureus</i>		
MSSA NRS72		
MRSA USA300-NRS384	BSL2 pathogen	
<b>Plasmids</b>		
pGEM T-easy	For TA cloning of MRSA <i>smpB-ssrA</i> , Amp <sup>r</sup>	
pET28a	Expression vector, IPTG-inducible, Kan <sup>r</sup>	
pCDR1	pGEM T-easy + MRSA USA300F <i>smpB-ssrA</i> , T7 promoter, Amp <sup>r</sup>	This study
pCDR2	pET28a + MRSA USA300F <i>smpB</i> , IPTG-inducible T7 promoter, Kan <sup>r</sup>	This study
PURExpress DHFR	Control plasmid included in PURExpress Kit (New England BioLabs)	

<b>Oligonucleotides</b>		
MRSA F2	5'-AAGTTGCTAGCAGCAATGAGGTGAGT-3'	This study
MRSA R2	5'-AAGTTGGTACCGCAATGCATTATCCC-3'	This study
smpBGibF	5'-GCCGCGCGCAGCCATATGGCTAAGAAGAAATCACC-3'	This study
smpBGibR	5'-CGGAGCTCGAATTCGTTAATAACGGGCTTTCATATCG-3'	This study
MRSAssrAF	5'-GGTACCGAAATTAATACGACTCACTATAGGGGACGTTTCATGGATTTCG-3'	This study
MRSAaarAR2	5'-TGGTGGAGACGGCGGGATTTGAACC-3'	This study
PURExpress Universal	5'-GAAATTAATACGACTCACTATAGGGAGACCACAACGGTTTCCCTCTA GAAATAATTTTGTTTAACTTTAAGAAGGAGATATACCA-3'	14
DHFR Rev UTR	5'-AAACCCCTCCGTTTAGAGAGGGGTTTTGCTAGTATCCGCCGCTCCAGAA TCTCAAAGCAA-3'	14
nsDHFR	PCR product from PURExpress DHFR	This study

**Table 5: Cell measurements**

	Membrane area	Membrane perimeter	Membrane roundness	Membrane max length	Membrane max breadth	Nucleoid area	Nucleoid perimeter	Nucleoid roundness	Nucleoid max length	Nucleoid max breadth	DAPI avg intensity	Sytox avg intensity	DAPI total intensity	Sytox total intensity
Water 12/4 A	261.8	64.0	0.8	22.3	15.4	119.4	43.5	0.8	15.9	9.4	6378.0	9519.6	764574.2	1154123.9
Water 12/4 B	257.1	63.6	0.8	22.2	15.2	108.0	41.5	0.8	15.3	8.9	7621.2	9389.1	842140.1	1055091.0
Water 12/11 C	267.8	65.4	0.8	23.0	15.2	106.5	41.7	0.7	15.2	9.0	7115.8	10110.4	794947.5	1190003.7
DMSO 12/4A	278.8	67.8	0.8	23.5	15.6	107.3	41.8	0.8	15.6	8.8	6147.9	9814.2	655981.9	1057379.1
DMSO 12/4B	238.7	61.5	0.8	21.0	14.9	109.6	41.7	0.8	15.0	9.4	6040.0	7728.7	678640.4	873074.4
DMSO 12/11C	253.0	64.6	0.8	22.6	15.2	106.1	41.3	0.8	15.2	8.9	5489.6	8365.8	589632.9	924359.8
EtOH 12/4 A	276.1	65.9	0.8	23.2	15.4	104.2	41.2	0.8	15.4	8.5	6850.3	10135.9	714665.3	1064440.2
EtOH 12/4B	252.5	63.0	0.8	22.0	15.1	104.8	41.2	0.8	15.3	8.6	8546.0	10887.8	881400.3	1137015.4
EtOH 12/11C	250.0	64.5	0.8	22.1	15.1	97.0	39.5	0.8	14.6	8.5	7145.0	10666.4	693195.8	1031643.5
Amp 12/4A	1422.9	220.6	0.4	91.7	21.3	590.5	164.4	0.3	73.1	12.0	5433.3	8898.0	3178381.0	5415652.5
Amp 12/4B	1215.7	189.2	0.4	80.0	20.5	478.7	154.3	0.3	68.1	11.3	7029.0	14669.4	3333282.6	7273676.2
Amp 12/11C	958.4	164.6	0.5	67.5	19.4	662.1	198.6	0.2	88.4	13.1	6919.4	7803.5	4664567.7	5504689.1
Rif 12/4A	347.5	75.2	0.8	26.8	16.8	136.1	48.5	0.7	18.3	9.5	4979.1	7679.2	680040.1	1126472.7
Rif 12/4B	351.1	75.6	0.8	27.2	16.4	119.1	44.5	0.7	16.9	8.6	9167.8	12646.2	1191217.9	1686870.5
Rif 12/11C	350.9	76.2	0.8	27.5	16.4	155.4	51.6	0.7	19.6	9.9	5663.8	8830.2	948957.8	1541625.7
Tet 12/4A	413.9	82.3	0.8	29.9	17.6	123.5	44.5	0.8	16.5	9.4	6475.1	11293.8	806607.6	1384006.5
Tet 12/4B	384.6	79.5	0.8	28.8	17.0	87.4	36.7	0.8	13.0	8.6	14926.8	28904.4	1337432.8	2524189.6
Tet 12/11C	417.2	83.7	0.7	30.9	17.1	78.6	34.9	0.8	12.3	8.2	10121.2	28609.9	782094.4	2327229.4
Cipro 12/4 A	1047.5	174.1	0.5	73.4	18.8	272.0	91.2	0.4	39.0	9.3	6196.1	7027.4	1707587.6	1945119.8
Cipro 12/4 B	1161.7	190.2	0.4	79.1	19.5	239.0	82.5	0.5	34.9	9.1	12114.7	9753.2	2944801.7	2392237.9
Cipro 12/11 C	924.8	159.2	0.5	66.6	18.0	185.9	74.0	0.5	31.3	8.2	11720.9	15162.9	2073250.2	2771241.9
Tric 12/4 A	323.8	78.9	0.7	28.0	15.9	194.2	63.0	0.6	24.5	10.3	7687.0	10450.7	1487743.5	2065231.7
Tric 12/4 B	383.2	83.7	0.7	31.0	16.6	178.3	60.3	0.6	23.5	9.8	14455.3	17143.1	2629344.4	3141230.1
Tric 12/11 C	349.9	80.3	0.7	28.7	16.6	201.7	64.8	0.6	25.2	10.4	12213.3	19561.1	2453799.3	3938226.1
Ctrlk 1	280.8	67.3	0.8	24.0	15.2	111.1	43.1	0.7	16.2	8.7	4621.2	11425.5	525336.9	1327634.6
KKL-10	287.5	67.8	0.8	24.0	15.6	115.5	43.1	0.8	15.9	9.3	5069.5	10360.5	596567.9	1230639.1
KKL-40	248.6	62.9	0.8	22.1	14.7	121.5	44.1	0.8	16.4	9.3	4032.2	12540.3	500937.9	1563657.7
KKL-55	235.9	61.5	0.8	21.8	14.0	102.5	40.6	0.8	15.0	8.6	5962.1	12488.5	655312.1	1326616.5
KKL-52	283.7	68.2	0.8	23.9	15.8	141.2	47.5	0.8	17.3	10.4	4208.0	13028.0	624306.6	1879219.5
KKL-35	223.4	59.7	0.8	21.1	13.7	115.8	43.0	0.8	15.7	9.5	4034.5	13453.5	485671.5	1567825.2
Ctrlk 2	259.3	64.5	0.8	23.2	14.6	120.3	44.8	0.7	16.8	9.0	6075.6	10823.1	758499.0	1331439.6
KKL-10 (2)	273.6	66.2	0.8	23.8	15.0	120.7	44.8	0.7	16.6	9.2	4545.1	8811.1	550791.6	1068196.4
KKL-52 (2)	265.4	65.3	0.8	23.3	14.8	94.8	39.6	0.7	14.8	8.1	5037.6	10853.3	494423.6	1054667.5
KKL-40 (2)	253.0	63.1	0.8	22.4	14.6	118.9	44.0	0.8	16.2	9.4	3873.1	7642.9	461490.9	929598.8
KKL-55 (2)	280.5	66.1	0.8	22.9	16.0	105.6	41.1	0.8	15.0	9.0	4083.1	8375.7	442131.7	914720.3
KKL-35 (2)	262.1	64.8	0.8	23.4	14.7	124.8	45.0	0.8	16.8	9.3	4298.5	11234.4	541350.1	1420458.6
Ctrlk 3	282.2	66.3	0.8	23.3	15.6	117.2	43.8	0.8	16.3	9.2	6620.6	12815.4	790496.3	1533836.3
KKL-10 (3)	270.2	65.7	0.8	22.7	16.0	93.6	38.5	0.8	13.9	8.6	5142.9	8607.9	484770.2	826016.9
KKL-52 (3)	272.0	65.3	0.8	22.7	15.7	115.6	43.0	0.8	15.6	9.4	7178.5	12005.5	818854.6	1410945.5
KKL-40 (3)	260.8	64.8	0.8	22.6	15.4	117.0	43.3	0.8	15.7	9.7	4222.1	8935.7	498421.3	1061907.0
KKL-55 (3)	335.0	73.8	0.8	26.0	17.0	134.5	46.5	0.7	17.3	9.5	6337.1	9256.4	848212.3	1336648.5
KKL-35 (3)	285.4	67.8	0.8	23.4	16.3	96.6	39.5	0.8	14.3	8.7	6556.3	8232.8	666305.2	819881.5

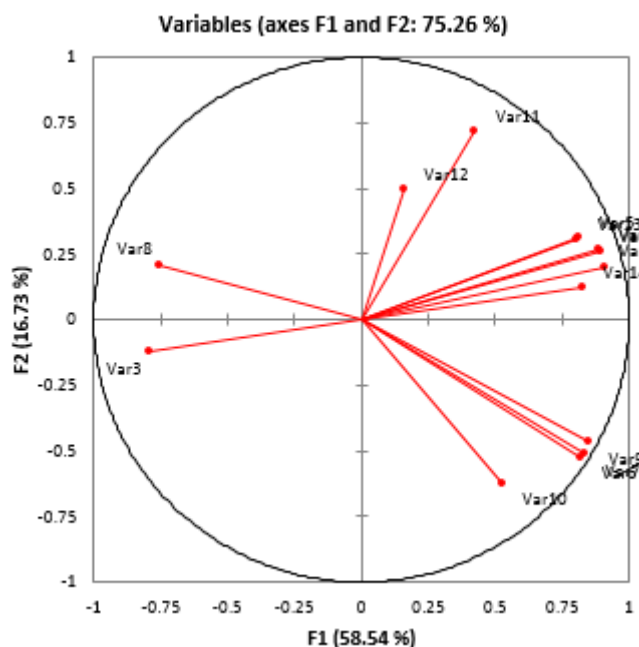


**Figure 8: Diagram of correlation between variables and factors.** This diagram shows each of the cell measurements in relation to the principal components F1 and F2. The measurements are linearly transformed into the principal components which are then used to create a two-dimensional scatter plot.

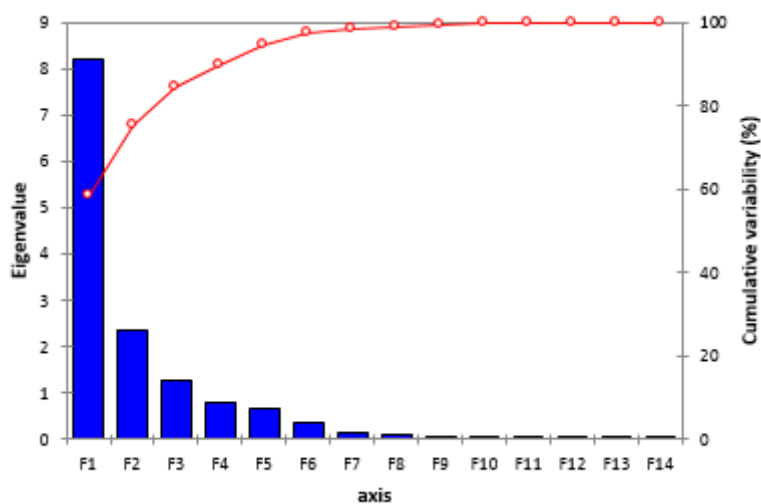


**Figure 9: Scree plot.** Eigenvalues associated with each factor are presented along with the cumulative variability associated with each.

## BIBLIOGRAPHY

1. Stark, Lisa. "Staphylococcus aureus: aspects of pathogenesis and molecular epidemiology." *Linköping University Medical Dissertations* 1371 (2013): 1 Web. 29 January 2015.
2. "MRSA and the Workplace" *Centers for Disease Control and Prevention*. Web. 23 January 2015.
3. "Diseases and Conditions: Staph infections" *Mayo Clinic*. Mayo Clinic Staff. Web. 29 January 2015.
4. "What is MRSA? How can MRSA be treated?" *Medical News Today*. Nichols, Hannah. Web. 3 February 2015.
5. "MRSA Infection" *emedicinehealth*. Davis, Charles Patrick. Stoppler, Melissa Conrad. Web 3 February 2015.
6. Klevens, R. Morrison, MA. Nadle, J. et al. "Invasive Methicillin-Resistant *Staphylococcus aureus* Infections in the United States." *JAMA*. 298.15 (2007): 1763-1771
7. "The silent epidemic: CA-MRSA and HA-MRSA" *American Association of Orthopaedic Surgeons*. Evans, Richard P. Web. 3 February 2015.
8. "Antibiotic Resistance Threats in the United States, 2013" *Centers for Disease Control and Prevention*. Web 3 February 2015.
9. "Unit 5: The emergence of antibiotic-resistant bacteria" *Annenberg Learner*. Web. Web 7 February 2015.
10. Livermore, David M. "Antibiotic resistance in staphylococci." *Int J Antimicrob Agents*. (2000): 1:S3-10.
11. Weigel, L. M. "Genetic Analysis of a High-Level Vancomycin-Resistant Isolate of *Staphylococcus aureus*." *Science*. 302.5650 (2003): 1569-571.
12. Chambers, Henry F. DeLeo, Frank R. "Waves of Resistance: *Staphylococcus aureus* in the Antibiotic Era." *Nat Rev Microbiol*. (2009) 7(9):629-641
13. Keiler, Kenneth C. and Nitya S. Ramadoss, "Bifunctional Transfer-messenger RNA." *Biochimie* 93.11 (2011): 1993-1997.

14. Ramadoss, N. S., J. N. Alumasa, L. Cheng, Y. Wang, S. Li, B. S. Chambers, H. Chang, A. K. Chatterjee, A. Brinker, I. H. Engels, and K. C. Keiler. "Small Molecule Inhibitors of *trans*-Translation Have Broad-spectrum Antibiotic Activity." *Proceedings of the National Academy of Sciences* 110.25 (2013): 10282-10287

15. "MRSA Infection Treatment" *emedicinehealth*. Davis, Charles Patrick. Stoppler, Melissa Conrad. Web 10 April 2015.

16. Nonejuie, P. Burkart, M. Pogliano, K. Pogliano, J. "Bacterial cytological profiling rapidly identifies the cellular pathways targeted by antibacterial molecules." *PNAS*. 110.40 (2013): 16169-16174

17. "Methods for Determining Bactericidal Activity of Antimicrobial Agents; Approved Guideline" *Clinical and Laboratory Standards Institute* (1999): Vol M26-A.

## ACADEMIC VITA

# Christopher D. Rae

*Curriculum Vitae*

301 S. Pugh Street, Apt. 404 | 570-660-9226 | rae.chris.d@gmail.com  
State College, PA 16801

## EDUCATION

**The Pennsylvania State University**  
Schreyer Honors College, Eberly College of Science  
Bachelor of Science in Biochemistry

**University Park, PA**  
Graduation: May 2015

## LEADERSHIP/VOLUNTEER EXPERIENCE

**Mount Nittany Medical Center**  
*Emergency Department Volunteer*

**June – December 2014**  
State College, PA

- Was responsible for patient transportation within the emergency department

**Penn State THON (Student run philanthropy fighting pediatric cancer)**  
*Operations Committee Member* (October 2014 – Present)

**September 2013 – Present**  
University Park, PA

- Setup and breakdown the venue for THON weekend
- Assist in yearlong fundraising and pediatric cancer awareness efforts

*Donor & Alumni Relations Committee Member* (October 2013 – February 2014)

- Assisted with THONvelope distribution, collection and sorting
- Guided donor and guest tours during THON weekend

**American Society for Microbiology Penn State Student Chapter**  
*President* (March 2014 – Present)

**September 2012 – Present**  
University Park, PA

- Lead officer meetings to assist in planning society functions
- Organize guest lectures, laboratory tours, scientific workshops, and faculty student mixers

*Event Coordinator* (March 2013 – 2014)

- Coordinated and organized social events and activities

## WORK EXPERIENCE

**Introductory Laboratory in Microbiology, Penn State University**  
*Teaching Assistant*

**January 2015 – Present**  
University Park, PA

- Guide first year students through basic microbiology laboratory protocols
- Demonstrate laboratory techniques and teach the theory behind them

**Dr. Kenneth Keiler Laboratory, Penn State University**

*Laboratory Undergraduate Researcher*

- Conduct undergraduate research on antibiotic resistance and development
- Project focus on identifying inhibitors of *trans*-translation in methicillin resistant *Staphylococcus aureus* (MRSA)

**May 2013 – Present**  
University Park, PA

**Avery Dennison Polymers Research & Development Laboratory**

*Laboratory Intern, Technician*

- Performed testing and research in the field of polymer chemistry and adhesives manufacturing
- Received Avery Dennison Safety Award for dedicated service and going above and beyond for safety

**Summers 2012, 2013**  
Mill Hall, PA

**Boy Scouts of America Camp Karoondinha**

*Rock Climbing/High Ropes Course Instructor*

- Directed program activities teaching children and teens skills in leadership and teamwork
- Instructed and supervised participants in the high ropes/rock climbing course
- Assisted in maintaining equipment inventories, safety, and advancement records

**Summers 2009 – 2011**  
Laurelton, PA

## HONORS

**American Society for Microbiology 2014 Undergraduate Research Fellowship**

- Funding to conduct full time summer research at Penn State University in Keiler Laboratory
- Invited to attend and submit an abstract at the 2015 ASM general meeting in New Orleans

**May 2014**

**Penn State Evan Pugh Scholar Award**

- Awarded to full-time junior or senior undergraduates in the top 0.5% of their class

**February 2014**

**Eagle Scout, Boy Scouts of America**

- Woolrich Troop 66, Susquehanna Council, North Woods District

**March 2008**

## PROFESSIONAL MEMBERSHIP

American Society for Microbiology

**October 2014 – Present**